tvst

Retina

Geometric Morphometrics Can Predict Postoperative Visual Acuity Changes in Patients With Epiretinal Membrane: A Retrospective Study

Sugao Miyagi[1], Akio Oishi[1], Eiko Tsuiki[1], and Takashi Kitaoka[1]

[1] Department of Ophthalmology and Visual Sciences, Graduate School of Biomedical Sciences, Nagasaki University, 1-7-1 Sakamoto, Nagasaki, Japan

Correspondence: Akio Oishi, Department of Ophthalmology and Visual Sciences, Graduate School of Biomedical Sciences, Nagasaki University, 1-7-1 Sakamoto, 852-8501 Nagasaki, Japan.
e-mail: akio.oishi@nagasaki-u.ac.jp

Received: September 26, 2022
Accepted: January 2, 2023
Published: January 24, 2023

Keywords: retina; epiretinal membrane; geometric morphometrics; optical coherence tomography; bending energy

Citation: Miyagi S, Oishi A, Tsuiki E, Kitaoka T. Geometric morphometrics can predict postoperative visual acuity changes in patients with epiretinal membrane: A retrospective study. Transl Vis Sci Technol. 2023;12(1):24, https://doi.org/10.1167/tvst.12.1.24

Purpose: To investigate the efficacy of the geometric morphometrics method for the evaluation of retinal deformation in patients with epiretinal membrane (ERM) and determine whether the degree of deformation can serve as a predictive factor for postoperative visual outcome.

Methods: We retrospectively evaluated data from 29 eyes of 29 patients with primary ERM. Preoperative optical coherence tomography images were compared with images of their normal fellow eyes using the geometric morphometrics thin-plate spline technique. Conventional parameters such as retinal layer thickness and previously reported indices were also measured. The correlation between the preoperative parameters and visual acuity was evaluated. Statistical comparisons were performed using a paired *t*-test, and associations between the optical coherence tomography image parameters and visual acuity were determined using Spearman's rank correlation coefficient.

Results: Bending energy, which was calculated using geometric morphometrics, was significantly associated with visual acuity as well as conventional optical coherence tomography parameters and previously reported indices. Multiple regression analysis showed that bending energy was an independent predictive factor for postoperative visual acuity changes.

Conclusions: The geometric morphometrics method is an effective approach for evaluating the severity of ERM and predicting the efficacy of surgery.

Translational Relevance: Geometric morphometrics can effectively evaluate retinal deformation in eyes with epiretinal membrane.

Introduction

Epiretinal membrane (ERM) is a vitreomacular disease characterized by a premacular fibrocellular membrane.[1] The pathologic change of ERM is characterized by wrinkling and distortion of the retina owing to membrane contraction. Although surgical removal is generally performed, improvement in visual acuity varies widely depending on the severity of ERM and retinal deformation.

Recent developments in optical coherence tomography (OCT) have enabled detailed and noninvasive assessment of retinal structures. Using this technology, studies have shown a correlation between preoperative OCT imaging parameters and visual acuity.[2] In these studies, OCT parameters included the thickness, integrity, or irregularity of each retinal layer.[3–6] These methods are simple, effective, and powerful tools for assessing ERM severity and retinal deformation. However, most of these parameters extract one-dimensional information from the OCT image. We believe that a two-dimensional OCT image information will offer an improved understanding for comprehensive analysis.

Geometric morphometrics is a biological approach to the quantitative investigation of differences in shapes between members of different species, such as insects

and fishes.[7] This approach can extract feature values while preserving the two-dimensional information by considering shape as coordinate information.[8] The thin-plate spline (TPS) method is a geometric morphometrics analysis technique that represents the deviation from a reference image as spatial distortion and calculates the bending energy required to create a warp.

In this study, we applied the TPS method to quantify retinal shapes in ERM while preserving the two-dimensional information and investigated correlation between geometric morphometrics parameter and visual acuity.

Materials and Methods

This retrospective study was conducted in accordance with the Declaration of Helsinki and approved by the Institutional Review Board of Nagasaki University Hospital Clinical Research Ethics Committee, Nagasaki, Japan. The ethics committee waived the need for written informed consent. Instead, the study information was published on the hospital's homepage. Patients were provided with the opportunity to opt out.

We screened patients who underwent surgery for idiopathic ERM at the Nagasaki University Hospital between January 2015 and December 2017. The exclusion criteria were high myopia (axial length > 26.0 mm or spherical equivalent < –6.0 diopters), secondary ERM (retinal vascular disease, retinal breaks, uveitis, and trauma), cataract Emery grade 3 or higher, a history of vitreoretinal surgery, and other ocular pathologies that may affect visual acuity (e.g., glaucoma and corneal opacity). In addition, patients with retinal disease in their fellow eye were excluded because the fellow eye was a reference for each patient. Visual acuity and OCT images were obtained preoperatively and at 1, 3, and 6 months postoperatively. Best-corrected visual acuity (BCVA) measured with the Landolt chart was converted to the logarithm of the minimum angle of resolution. Preoperative and postoperative OCT scans were obtained using a Cirrus HD-OCT (Carl Zeiss Meditec, Dublin, CA). Surgical procedures were performed using standard 25G pars plana vitrectomy under sub-Tenon anesthesia. All phakic eyes underwent phacoemulsification and intraocular lens implantation. After core vitrectomy, the ERM was removed using intraocular forceps. Internal limiting membrane peeling was performed at the surgeon's discretion. Triamcinolone acetonide and Brilliant Blue G were used for intraoperative visualization.

The thickness of the retinal layers was measured by manual image analysis using ImageJ software (National Institutes of Health, Bethesda, MD). We also measured the central foveal thickness (CFT), foveal photoreceptor outer segment length, juxtafoveal (500 µm apart from the foveola) ganglion cell layer (GCL) thickness, juxtafoveal inner nuclear layer (INL) thickness, and juxtafoveal outer nuclear layer thickness. The CFT was defined as the distance between the vitreoretinal interface and the retinal pigment epithelium cell line at the centre of the fovea. The photoreceptor outer segment length was defined as the distance between the ellipsoid zone and the retinal pigment epithelium. Juxtafoveal GCL, INL, and outer nuclear layer thicknesses were measured at 500 µm from the fovea. The photoreceptor deformation index and inner retinal irregularity index were determined, as previously reported.[4,5] Govetto's grading system was used to classify ERM staging.[9] The segmentation and grading of OCT images were performed by two retinal specialists. In case of different judgment, decision was made by discussion.

Geometric morphometrics analysis (TPS, semilandmark method) was performed using freely available software[10] (TPS series: tpsDig2, tpsSplin). Landmarks were set at every 100 µm up to a distance of 1000 µm from the foveola at the boundary of the internal limiting membrane and retinal pigment epithelium. The boundaries of the INL were marked at every 100 µm up to a distance of 1000 µm from the innermost point of the INL. Normal retinal shape of the fellow eye was used as a reference image, and bending energy was calculated in pre- and postoperative ERM images (Fig. 1).

Furthermore, bending energy was calculated with different settings for the reference image and reference point to ensure robustness of the analysis (Fig. 3). First, we used a single normal retinal image as the reference image, whereas each fellow eye was used in the main study (Fig. 3A). Second, bending energy was calculated at different intervals of 200 and 500 µm from the reference points and 100 µm in the main study (Fig. 3B).

Statistical analyses were performed using EZR software (version 1.40, Jichi Medical University, Shimotsuke, Japan), which is a modified version of R commander.[11] Statistical comparisons were performed using a paired *t*-test. Associations between OCT image parameters and visual acuity were determined using Spearman's rank correlation coefficient. A multiple regression analysis was performed using the Akaike information criterion for variable selection. Data are presented as mean ± standard deviation. A *P* value of less than 0.05 was considered statistically significant.

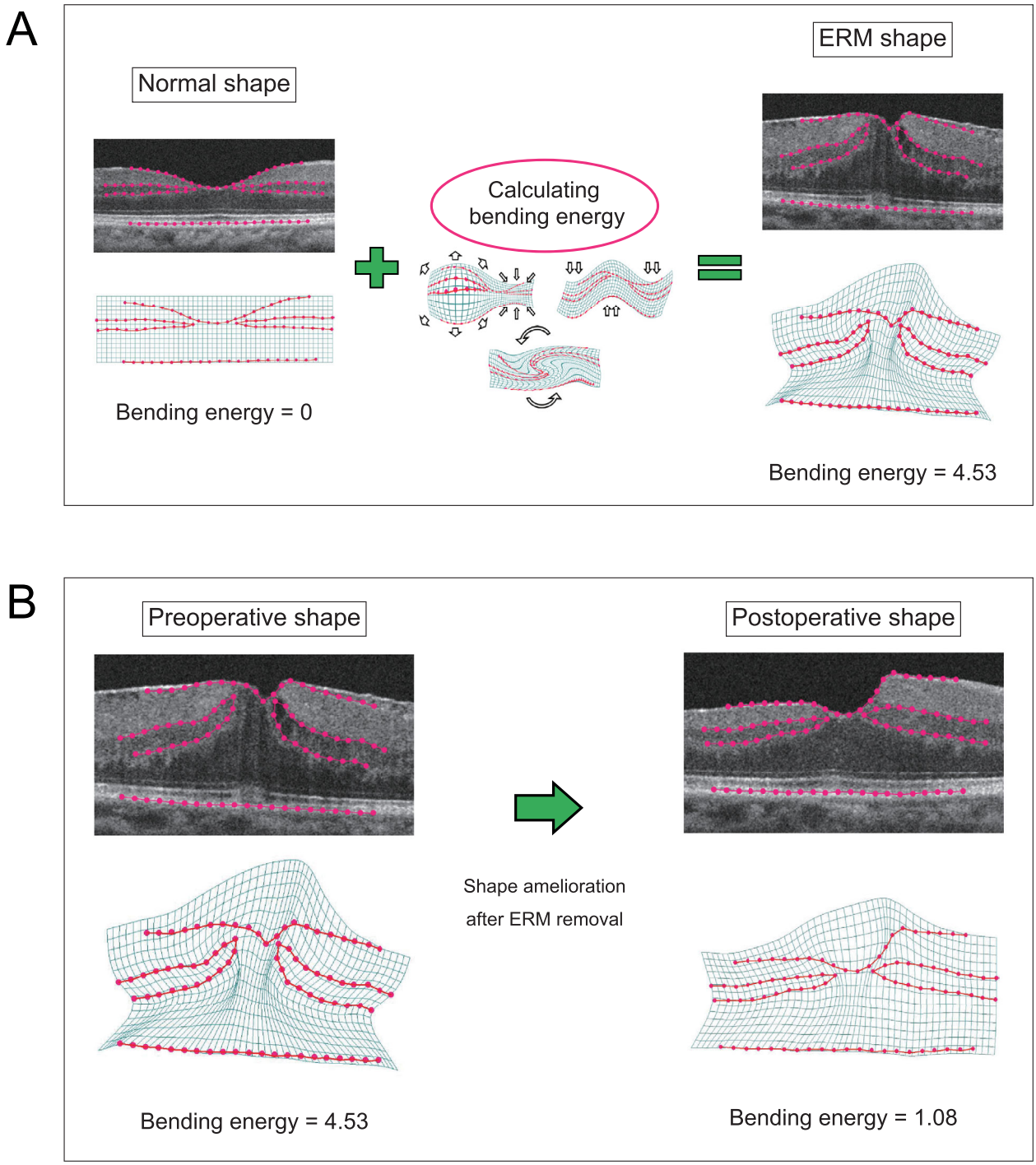

Figure 1. Method of converting deformation of the retina into spatial distortions in eyes with ERM. (**A**) In the TPS method, deformation of the retina is regarded as distortion of the coordinate plane in which the retinal image is plotted, and the energy required for the distortion (bending energy) is calculated. Retinal image of the normal fellow eye is used as reference (bending energy = 0). (**B**) As the retinal shape improves with surgical ERM removal, bending energy also decreases.

Results

Twenty-nine eyes of 29 patients were included in this study. Surgeries were performed by two surgeons. The clinical characteristics at baseline and 6 months postoperatively are shown in Table 1. The mean BCVA significantly improved after surgery. The thickness of retinal layers (CFT, GCL, and INL) significantly decreased. The bending energy was also significantly

Table 1. Basic Characteristics of Patients With ERM

Characteristic	Preoperative	Six Months Postoperatively	*P* Value
No. of eyes/patients	29/29	–	–
No. of men/women	7/22	–	–
Age, years	69.4 ± 6.7	–	–
BCVA, logMAR	0.269 ± 0.139	0.036 ± 0.117	<0.0001*
CFT	403 ± 89	305 ± 60	<0.0001*
GCL	130 ± 32	86 ± 20	<0.0001*
INL	84 ± 22	71 ± 11	0.00437*
ONL	176 ± 22	177 ± 14	0.75
PROS	53 ± 12	54 ± 6	0.884
Bending energy	8.67 ± 4.79	4.55 ± 2.38	<0.0001*
ILM peeling (+/−)	26/3	–	–
Cataract surgery (+/−)	27/2	–	–
ERM staging			
Stage 1 (n, %)	6 (21)		
Stage 2 (n, %)	19 (66)		
Stage 3 (n, %)	4 (14)		
Stage 4 (n, %)	0 (0)		

Data are mean ± standard deviation unless otherwise noted.

*Statistically significant at $P < .05$ by paired *t*-test.

ILM, internal limiting membrane; logMAR, logarithm of the minimum angle of resolution; ONL, outer nuclear layer; PROS, photoreceptor outer segment.

reduced. For ERM staging, stages 1 and 2 cases were commonly included in our study and stage 3 cases were rare, stage 4 cases were not included in this study.

Table 2 shows correlations between the preoperative parameters and BCVA (preoperative, postoperative, and change from baseline to 6 months postoperatively). The preoperative BCVA had significant correlations

Table 2. Correlation Among Preoperative Parameters and Visual Acuity

Preoperative Parameter	Preoperative BCVA	BCVA 6 Months Postoperatively	BCVA Change
BCVA	–	$r = .598$	$r = -0.519$
		$P = .000607$*	$P = 0.00395$*
Age	$r = 0.37$	$r = 0.671$	$r = 0.163$
	$P = 0.0479$*	$P < 0.0001$*	$P = 0.397$
CFT	$r = 0.287$	$r = 0.019$	$r = -0.399$
	$P = 0.132$	$P = 0.922$	$P = 0.032$*
GCL	$r = 0.41$	$r = 0.236$	$r = -0.332$
	$P = 0.0273$*	$P = 0.218$	$P = 0.0789$
INL	$r = 0.327$	$r = 0.0846$	$r = -0.379$
	$P = 0.0829$	$P = 0.663$	$P = 0.0427$*
ONL	$r = -0.213$	$r = -0.186$	$r = 0.268$
	$P = 0.268$	$P = 0.334$	$P = 0.161$
PROS	$r = -0.348$	$r = -0.196$	$r = 0.117$
	$P = 0.064$	$P = 0.309$	$P = 0.544$
Bending energy	$r = 0.561$	$r = -0.0179$	$r = -0.74$
	$P = 0.00156$*	$P = 0.926$	$P < 0.0001$*

*$P < .05$ (Spearman's rank correlation coefficient).

ONL, outer nuclear layer; PROS, photoreceptor outer segment.

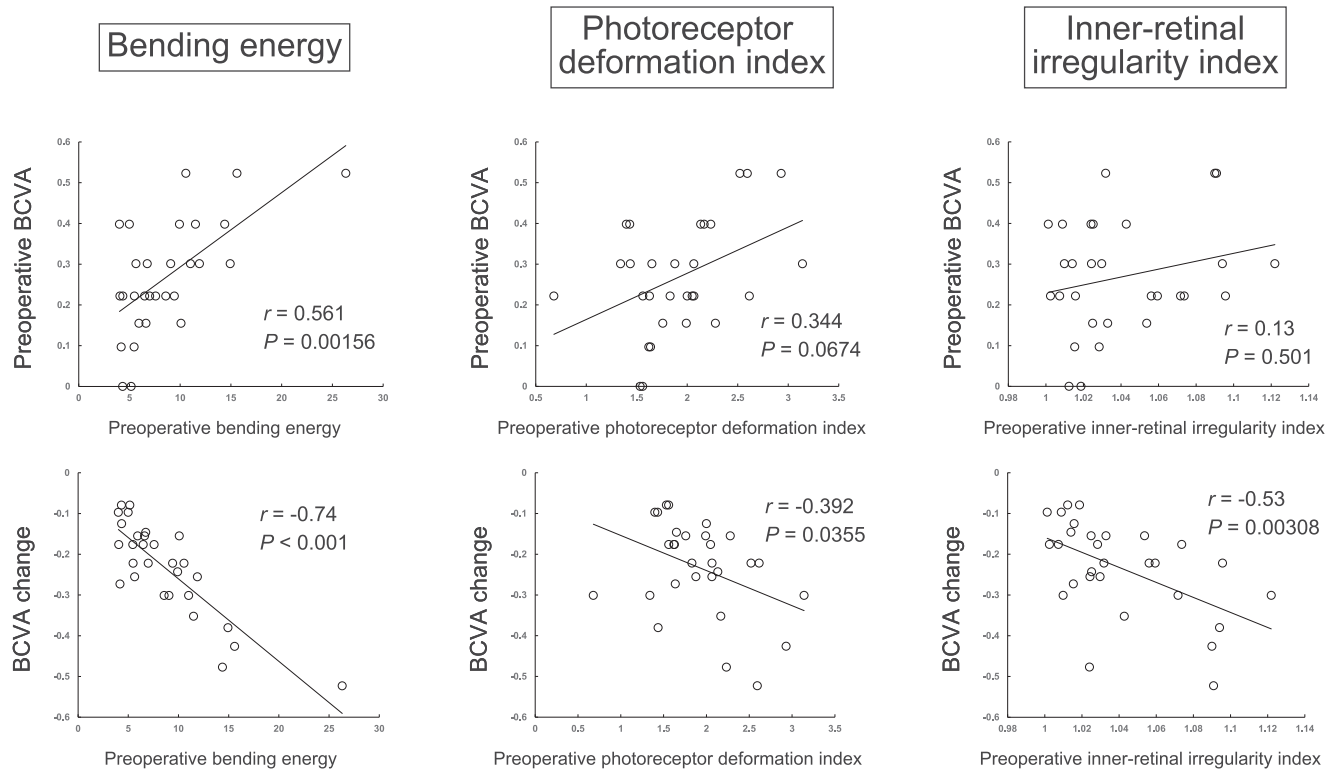

Figure 2. Comparison of bending energy and previously reported indices for the evaluation of visual function in eyes with ERM. Correlations between visual acuity and preoperative retinal parameters (bending energy and reported indices) are presented. Bending energy is correlated with visual acuity no less than previously reported indices. The Spearman's rank correlation coefficient was used for statistical analysis.

Table 3. Multiple Regression Analysis Between Preoperative Parameters and Postoperative Visual Acuity Change in Patients With ERM

Preoperative Parameter	Standard Regression Coefficient	*P* Value
Age	0.280	0.01733
BCVA	−0.284	0.05478
Bending energy	−0.661	<0.0001
		Adjusted $R^2 = 0.7517$

Variable selection was performed using the Akaike information criterion.

with baseline age, GCL, and bending energy and weak correlations and marginal *P* values with the remaining factors. Meanwhile, postoperative BCVA significantly correlated with preoperative BCVA and age. Regarding change in BCVA, poor preoperative BCVA, thick CFT, thick INL, and larger bending energy were associated with better improvement.

Next, we used multiple regression analysis because these parameters are correlated each other. Table 3 shows the results of multiple regression analysis between BCVA change and preoperative parameters (age, preoperative BCVA, preoperative OCT parameters). The thickness of the central fovea and INL were not selected as contributing factors despite the univariate correlation. Meanwhile, preoperative bending energy was significantly related to BCVA change.

Finally, we compared the correlation coefficients between visual acuity and bending energy to those of the previously reported indices. Figure 2 shows the correlations between previously reported indices of patients with ERM and BCVA (preoperative, change). Bending energy showed a similar correlation coefficient as the reported indices.

Additionally, we verified the robustness of our geometric morphometrics parameters to the reference setting. For one variation, we calculated bending energy using only one randomly chosen reference OCT image (Fig. 3A). The pilot analysis showed correlation coefficients comparable to those of the patient-specific analysis. In another variation, we performed the analysis with different spacings of the reference points (200 and 500 µm) (Fig. 3B). Although the correlation coefficient tended to be smaller with a larger reference point spacing, the correlation between bending

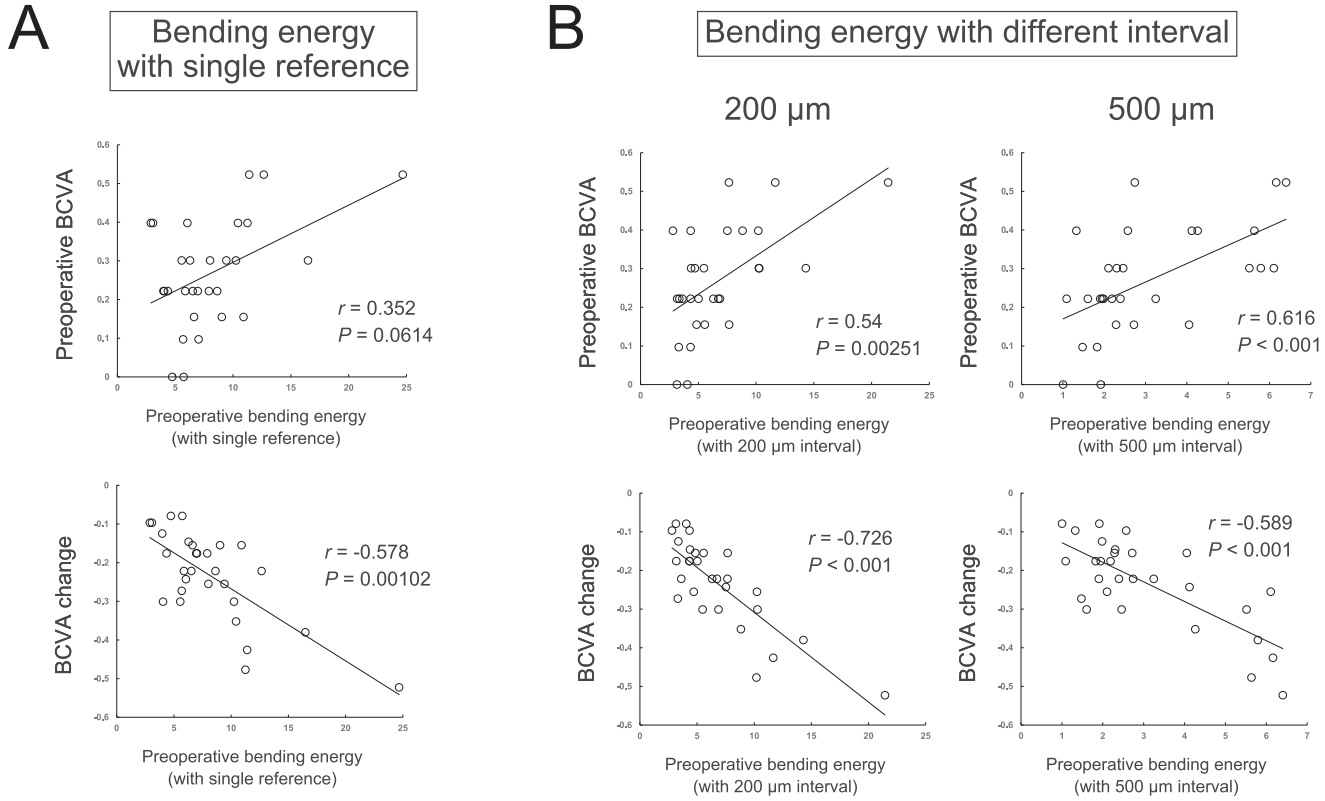

Figure 3. Robustness verification of bending energy by different measurement. To verify robustness of bending energy by variations in measurement technique, bending energy was calculated with different method of setting reference image and reference point. (**A**) A single normal retinal image was regarded as the reference image, whereas each fellow eye was used in the main study. (**B**) Bending energy was calculated with different interval of reference points (200 µm and 500 µm), whereas it was 100 µm in the main study. The Spearman's rank correlation coefficient was used for statistical analysis. BCVA, best corrected visual acuity.

energy and visual acuity was still observed at all spacings.

Discussion

In the present study, we applied geometric morphometrics to ERM analysis. Previous studies have applied geometric morphometrics in ophthalmology to investigate disc shape in glaucoma and extraocular muscle position in strabismus.[12–15] However, to the best of our knowledge, this technique has not been used in the analysis of ERM. For the first time, we calculated bending energy to quantify retinal shape deformation and showed that this factor is a significant predictor of visual outcome.

The advantage of geometric morphometrics is its ability to consider two-dimensional information of OCT images instead of one-dimensional nature of distance parameters. Retinal layer thickness is a simple and easy-to-use indicator of ERM severity. However, there are limitations in evaluating distortion in OCT images using one-dimensional parameters, considering that the original image inherently contains two-dimensional information. Regardless of the severity of the distortion, retinal thickening is limited by the plasticity of the organ. Thus, conventional parameters may underestimate the differences among the most severe ERM cases. In contrast, as the distortion increases, bending energy can theoretically increase without limit. In our study, bending energy showed a wider variance than conventional parameters, indicating a larger effective measurement range of analysis than conventional parameters. This finding partly explains the strong correlation between bending energy and visual acuity.

Because this is the first attempt to apply geometric morphometrics to the evaluation of ERM, we assessed the robustness of the analysis (Fig. 3). Briefly, the analysis worked well with a random normal eye as well as a healthy fellow eye, and decreasing the number of sampling points did not affect the correlation. These results indicate the robustness of this method to the

variations in reference settings. Furthermore, these results may also suggest the possibility of automating the analysis. Robustness against reduction of reference points and no necessity of a healthy fellow eye would be an advantageous property for automated analysis by software. It may be possible to make this method part of the built-in function of OCT measurement equipment, and then, it can be a practical too in busy routine clinical care. Hence, we believe that our method can be reliably used in future studies to replicate the results. For instance, it can effectively quantify other retinal diseases based on changes in the OCT images. Because ERM is characterized by the deformation of the retinal shape, we used this method effectively to investigate patients with ERM in this study. However, this method can be applied to any disorder by setting the reference points on the OCT image.[15] Moreover, other geometric morphometrics techniques could effectively evaluate retinal shape. For example, the elliptic Fourier descriptor method can quantify the contour of a closed curve by approximating it as a composite of trigonometric functions. Using such methods may enable quantification of lesions that are otherwise difficult to analyze using conventional methods. Now that we can obtain detailed retinal images, most of the information contained in the image can help in better patient management. Thus, geometric morphometrics is an effective upgrade over conventional image evaluation methods in ophthalmology.

This study, however, had some limitations. First, this method does not reflect specific retinal findings investigated in previous studies,[16] such as schisis[17] and ellipsoid zone disruption,[18,19] because the analysis converts all shape distortions equally to bending energy. Adjusting the weights for visually important findings may improve the accuracy of the prediction. Second, this method requires well-defined retinal layers for calculating bending energy. Thus, severe ERM cases such as Govetto's stage 4 would be difficult to be evaluated by this method. However, as long as the retinal layers can be defined, it may be an effective tool to evaluate the degree of ERM. Third, patients with retinal diseases in both eyes had to be excluded because their fellow eyes were used as controls. However, the preliminary results (Fig. 3) indicate that the image of the fellow eye is not required for analysis. Establishing standard morphological data from a large dataset representing specific age, sex, and axial length would eliminate the need to use fellow eyes. Fourth, the number of cases included in this study was relatively small. Further studies would be desired to validate the effectiveness of this method. Fifth, cataracts may affect the visual acuity. However, we selected the cases with mild cataract to minimize the effect. Indeed, the visual acuity of all fellow eye with cataract was better than 0.2 (logarithm of the minimum angle of resolution). Furthermore, simultaneous vitrectomy and cataract surgery was majority in this study (93%). Thus, we think the effect of cataract in this study was relatively small. Finally, because the TPS method can be potentially developed into three dimensions,[20] using a three-dimensional image dataset obtained with OCT volume scan would make the analysis more robust.

In summary, we devised an approach to calculate the novel retinal deformation index using geometric morphometrics analysis and established this index as a predictive factor for visual outcomes. Thus, our findings have paved a way for future studies to confirm the validity of this approach.

Acknowledgments

Disclosure: **S. Miyagi**, None; **A. Oishi**, Santen Pharmaceutical (R), Novartis Pharma (R), Bayer Yakuhin (R), Amgen (R), Senju (R); **E. Tsuiki**, Bayer Yakuhin (R), Novartis Pharma (R), Alcon Japan (R); **T. Kitaoka**, Alcon Japan (F), Santen (F), Senju (F), Alcon Japan (R), Novartis Pharma (R), Senju (R), Santen (R), Bayer Yakuhin (R)

References

1. Sebag J. Vitreous: in health and disease. New York: Springer; 2014.
2. Scheerlinck LM, van der Valk R, van Leeuwen R. Predictive factors for postoperative visual acuity in idiopathic epiretinal membrane: a systematic review. *Acta Ophthalmol*. 2015;93:203–212.
3. Kim JH, Kang SW, Kong MG, Ha HS. Assessment of retinal layers and visual rehabilitation after epiretinal membrane removal. *Graefes Arch Clin Exp Ophthalmol*. 2013;251:1055–1064.
4. Hosoda Y, Ooto S, Hangai M, Oishi A, Yoshimura N. Foveal photoreceptor deformation as a significant predictor of postoperative visual outcome in idiopathic epiretinal membrane surgery. *Invest Ophthalmol Vis Sci*. 2015;56:6387–6393.
5. Cho KH, Park SJ, Cho JH, Woo SJ, Park KH. Inner-retinal irregularity index predicts postoperative visual prognosis in idiopathic epiretinal membrane. *Am J Ophthalmol*. 2016;168:139–149.
6. Shimozono M, Oishi A, Hata M, et al. The significance of cone outer segment tips as a prognostic factor in epiretinal membrane surgery. *Am J Ophthalmol*. 2012;153:698–704, 704 e691.

7. Cooke SB, Terhune CE. Form, function, and geometric morphometrics. *Anat Rec (Hoboken)*. 2015;298:5–28.
8. Kendall D. The diffusion of shape. *Adv Appl Probab*. 1977;9:428–430.
9. Govetto A, Lalane RA, Sarraf D, Figueroa MS, Hubschman JP. Insights into epiretinal membranes: presence of ectopic inner foveal layers and a new optical coherence tomography staging scheme. *Am J Ophthalmol*. 2017;175:99–113.
10. Rohlf FJ. The tps series of software. *Hystrix, the Italian J Mammal*. 2015;26:9–12.
11. Kanda Y. Investigation of the freely available easy-to-use software 'EZR' for medical statistics. *Bone Marrow Transplant*. 2013;48:452–458.
12. Sanfilippo PG, Cardini A, Hewitt AW, Crowston JG, Mackey DA. Optic disc morphology–rethinking shape. *Prog Retin Eye Res*. 2009;28:227–248.
13. Touze R, Heuze Y, Robert MP, et al. Extraocular muscle positions in anterior plagiocephaly: V-pattern strabismus explained using geometric morphometrics. *Br J Ophthalmol*. 2020;104:1156–1160.
14. Sibony PA, Wei J, Sigal IA. Gaze-evoked deformations in optic nerve head drusen: repetitive shearing as a potential factor in the visual and vascular complications. *Ophthalmology*. 2018;125:929–937.
15. Gampa A, Vangipuram G, Shirazi Z, Moss HE. Quantitative association between peripapillary Bruch's membrane shape and intracranial pressure. *Invest Ophthalmol Vis Sci*. 2017;58:2739–2745.
16. Watanabe K, Tsunoda K, Mizuno Y, Akiyama K, Noda T. Outer retinal morphology and visual function in patients with idiopathic epiretinal membrane. *JAMA Ophthalmol*. 2013;131:172–177.
17. Lam M, Philippakis E, Gaudric A, Tadayoni R, Couturier A. Postoperative outcomes of idiopathic epiretinal membrane associated with foveoschisis. *Br J Ophthalmol*. 2021;106:1245–1251.
18. Suh MH, Seo JM, Park KH, Yu HG. Associations between macular findings by optical coherence tomography and visual outcomes after epiretinal membrane removal. *Am J Ophthalmol*. 2009;147:473–480.e473.
19. Itoh Y, Inoue M, Rii T, Hirota K, Hirakata A. Correlation between foveal cone outer segment tips line and visual recovery after epiretinal membrane surgery. *Invest Ophthalmol Vis Sci*. 2013;54:7302–7308.
20. Polly PD, Motz GJ. Patterns and processes in morphospace: geometric morphometrics of three-dimensional objects. *Paleontological Society Papers*. 2017;22:71–99.